Discover Oncology

Research

SMAD4 mutation drives gut microbiome shifts toward tumor progression in colorectal cancer

Travis J. Gates[1] · Dechen Wangmo[1] · Kyra M. Boorsma Bergerud[2] · Bridget M. Keel[2] · Christopher Staley[2,3] · Subbaya Subramanian[2,3,4]

Received: 27 January 2025 / Accepted: 5 May 2025
Published online: 09 October 2025

Abstract

Background Colorectal cancer (CRC) progression is driven by a series of sequential mutations in key driver genes; however, the factors underlying tumor progression and metastasis remain poorly understood. Mutations in TP53 and SMAD4, in particular, are associated with CRC progression. Although gut microbiome dysbiosis is implicated in CRC initiation and progression, the interactions between the microbiome and specific CRC driver mutations, especially those promoting metastasis, are not well defined.

Methods In this study, we utilized triple mutant (Apc, Kras, Tp53; AKP) and quadruple mutant (Apc, Kras, Tp53, Smad4; AKPS) organoid-based orthotopic mouse models of CRC to investigate the impact of the SMAD4 mutation on microbiome composition.

Results Our results reveal significant differences in metastatic potential and microbial community dynamics between the two tumor models. AKPS tumors exhibited metastasis to the lymph nodes, liver, and lungs, while AKP tumors remained confined to the colon. Longitudinal microbiome analysis showed shifts in microbial composition within each tumor model. Both AKP and AKPS models demonstrated enrichment of *Faecalibaculum* and a decrease in *Dubosiella* over time; however, additional shifts were noted with distinct taxa associated with late-stage tumors in each group. Notably, the AKPS model exhibited higher relative abundances of pro-inflammatory taxa, including *Turicibacter, Romboutsia, and Akkermansia*, suggesting that the SMAD4 mutation promotes a more immunosuppressive and pro-metastatic microbiome profile.

Conclusions These findings emphasize the significance of SMAD4 mutation and microbiome modulation, revealing the interaction between host genetics and gut microbiota in driving colorectal cancer aggressiveness and suggesting potential microbial targets.

Keywords Gut microbiome · SMAD4 · Driver gene mutations · Colorectal cancer · Metastasis

Supplementary Information The online version contains supplementary material available at https://doi.org/10.1007/s12672-025-02580-6.

✉ Subbaya Subramanian, subree@umn.edu; Travis J. Gates, gates173@umn.edu; Dechen Wangmo, wangm005@umn.edu; Kyra M. Boorsma Bergerud, boors011@umn.edu; Bridget M. Keel, keel@stanford.edu; Christopher Staley, cmstaley@umn.edu | [1]Department of Pharmacology, University of Minnesota Medical School, Minneapolis, MN, USA. [2]Department of Surgery, University of Minnesota Medical School, 11-212 Moos Tower, Mayo Mail Code 195, 420 Delaware Street SE, Minneapolis, MN 55455, USA. [3]Masonic Cancer Center, University of Minnesota Medical School, Minneapolis, MN, USA. [4]Center for Immunology, University of Minnesota Medical School, Minneapolis, MN, USA.

1 Introduction

Colorectal cancer (CRC) is the third most commonly diagnosed cancer and the third leading cause of cancer-related deaths in the United States [1]. Although the global incidence of CRC is declining, early-onset CRC, defined as CRC occurring in individuals under 50, has steadily increased [1–3]. This trend has resulted in revised screening guidelines, with colonoscopy now recommended starting at age 45 [4]. Despite similarities in the genetic mutations found in early- and late-onset CRC, patients with early-onset CRC often experience significantly poorer survival rates [5, 6].

The etiology and oncogenic transformation of CRC involve sequential mutations in key driver genes, such as *APC, KRAS, TP53, and SMAD4*.[7] Mutations in the tumor suppressor APC lead to cellular overgrowth and polyp formation [8]. Oncogenic mutations in KRAS promote uncontrolled cell proliferation and resistance to treatment [9, 10]. TP53 mutations prevent apoptosis in damaged cells, allowing them to proliferate [11, 12]. The loss of SMAD4 disrupts normal TGF-β-mediated epithelial regulation, leading to uncontrolled proliferation, impaired differentiation, and the activation of epithelial-to-mesenchymal transition (EMT), which promotes tumor metastasis [13, 14].

While genetic mutations primarily drive CRC, tumor-extrinsic factors such as diet and the gut microbiome significantly influence its progression. A diet high in fat and sugar has been strongly associated with CRC [15, 16], with microbiome dysbiosis playing a central role [17, 18]. Dysbiosis, characterized by an increase in pathogenic, cancer-promoting bacteria and a decrease in protective species, can disrupt gut barrier function and support a pro-inflammatory environment, thus promoting CRC development [19]. Species like *Bacteroides* are implicated in this process by compromising the intestinal barrier and facilitating tumorigenesis [20, 21].

Microbiome alterations are crucial not only for CRC initiation but also for its progression. For instance, *Fusobacterium* has been associated with alterations in the *ATM* gene, which regulates TP53 expression [22]. KRAS mutations show positive correlations with *Faecalibacterium* and negative correlations with *Bifidobacterium* and *Lachnospiraceae* [23], while APC mutations are associated with a reduced abundance *of Faecalibacterium* and *Bifidobacterium* [24]. Inactivation of SMAD4 has been linked to decreased *Bacteroides* and increased chemoresistance [25].

Despite these findings, the longitudinal relationship between the gut microbiome and the accumulation of CRC driver mutations remains underexplored. To address this gap, we used a triple mutant (*Apc, Kras, p53*; AKP) and a quadruple mutant (*Apc, Kras, p53, Smad4*; AKPS) organoid-based orthotopic CRC model to examine microbiome alterations during tumor progression. Mice with AKPS tumors developed liver metastases in 8 weeks, while AKP tumors remained localized to the colon. This differential tumor behavior prompted us to explore how the presence or absence of SMAD4 might influence the microbial environment and contribute to the metastatic burden. Our findings reveal significant compositional differences in the microbiome between AKP and AKPS mice, with both groups showing increased *Faecalibaculum* as tumors progressed. Conversely, *Dubosiella* was depleted in both groups. Furthermore, *Akkermansia* exhibited inverse trends in abundance, decreasing in AKP mice but increasing in AKPS mice. These results highlight potential microbial factors critical to CRC progression and metastasis.

2 Materials and methods

2.1 Organoid generation

C57BL/6 mice harboring mutations in *Apc* and *Kras* were used to generate AKP and AKPS organoids for tumor implantation (AKP and AKPS kindly provided by Dr. Westcott). Briefly, the colons were dissected and treated with 10 mM EDTA (cat#: AM9260G, Invitrogen, Waltham, MA) to isolate crypt cells, following the protocol described by Sato et al. [26] The isolated crypts were resuspended in Matrigel (cat#: 354234, Corning, Corning, NY) to support their growth. To create AKP organoids, CRISPR-Cas9 technology was employed to knockout the *p53* gene in the isolated crypt cells. For AKPS organoids, both the *p53* and *Smad4* genes were targeted for knockout using CRISPR-Cas9. The genetically modified crypt cells were cultured in Matrigel, allowing them to form organoids before transplantation.

2.2 Animal husbandry

Based on prior studies, we estimated a moderate effect size Cohen's d = 0.8 with a significance level (α) of 0.05 and a statistical power of 0.8. Using these parameters, a minimum of 8 mice per group was required to detect statistically significant differences. To ensure sufficient power for assessing longitudinal microbiome changes while accounting for biological variability, we included 9 mice in our study. Female C57BL/6 mice (n = 9), aged 6 to 8 weeks, were obtained from The Jackson Laboratory. Upon arrival, the mice were individually housed to eliminate potential environmental variations from group housing and to ensure consistent conditions throughout the study. The mice were then subjected to an endoscopy-guided injection of AKP or AKPS organoids. Stool samples were collected weekly for the duration of the 8-week study period. At the end of week 8, the mice were euthanized, and their colons were harvested, fixed, and processed for histopathological analysis.

Ethics statement: The animal use protocol (2209-40412A) was approved by the Institutional Animal Care and Use Committee (IACUC) in compliance with the IACUC Policy on the Principal Investigator's Role in Animal Research. Further details are available at IACUC Animal Use Guidelines. (https://research.umn.edu/units/iacuc/policies-guidelines/animal-use-guidelines-exceptions) All animals were euthanized using the CO2 inhalation method, as recommended by the Panel on Euthanasia of the American Veterinary Medical Association.

2.3 Endoscopy guided injection

In vivo high-resolution colonoscopies were conducted using the Mainz Coloview mini-endoscopic system (Karl Storz Endoskope, Tuttlingen, Germany) during orthotopic tumor cell implantation. Mice were anesthetized with 4% isoflurane administered via inhalation, and atropine (0.04 mg/kg) was given intraperitoneally to decrease colon motility, contraction, and secretion during the injection procedure. Each AKP group received 5000 Apc/Kras/p53 organoids as dissociated cells, while the AKPS group was injected with 5000 Apc/Kras/p53/SMAD4 cells. After implantation, the mice were placed on a heating pad to support recovery.

2.4 Longitudinal fecal sample collection

Fecal samples were collected longitudinally once per week for a period of 8 weeks. Mice were transferred to autoclaved, SPF (specific pathogen-free) cages without food or bedding, where they were allowed to remain for one hour to facilitate fecal pellet production. During the collection period, 3 to 5 fecal pellets were harvested from each mouse. Following sample collection, mice were returned to their individual housing. Stool samples were pooled by the experimental group and stored at −80 °C until DNA isolation and further processing.

2.5 Histopathological analysis

At the experimental endpoint, mouse colons were fixed overnight in 10% neutral-buffered formalin. After fixation, tissues were transferred to 70% ethanol and submitted to the Clinical and Translational Sciences Institute at the University of Minnesota for further processing. The tissues were paraffin-embedded, and two sections from each mouse were stained with hematoxylin and eosin. Board-certified pathologists subsequently reviewed the stained sections for the presence of dysplasia and both acute and chronic inflammation.

2.6 Fecal DNA extraction and 16S amplicon sequencing

Approximately 0.1 g of mouse fecal pellets were homogenized and processed for DNA extraction using the PowerSoil DNA Isolation Kit (Qiagen) with the QIACube automated platform, following the manufacturer's Inhibitor Removal Technology (IRT) protocol. The V4 hypervariable regions of the 16S rRNA gene were amplified using the 515F/806R primer set and sequenced. Negative controls, including sterile water and no-template controls, were included to ensure the absence of contamination, and no amplicons were detected.

Paired-end sequencing of the amplicons was performed on the MiSeq platform (Illumina, Inc., San Diego, CA, USA), generating 301 nucleotide (nt) reads. All sequence processing was conducted using Mothur software (version 1.48.0) [27]. Raw Fastq files were trimmed to 150 nt to remove low-quality regions and merged using the Fastq-join function [28]. Sequence reads with mean quality scores <35 over a 50-nt window, homopolymers > 8 nt, ambiguous bases, or

mismatches to primer sequences (more than 2 nt) were discarded. High-quality sequences were aligned to the SILVA database (ver. 132) [29] and subjected to a 2% pre-clustering step to remove likely sequencing errors [30]. Chimeric sequences were identified and removed using the UCHIME package [31]. Operational Taxonomic Units (OTUs) were clustered at 99% similarity using the complete-linkage algorithm. Taxonomic assignments were made using the Ribosomal Database Project (ver. 16) [32].

The Raw Fastq files are available at https://www.ncbi.nlm.nih.gov/sraPRJNA988535.

2.7 Bioinformatics and data analysis

Alpha diversity of the microbial communities was assessed using the Shannon and Chao1 indices. Beta diversity was evaluated using Principal Coordinate Analysis (PCoA) based on Bray–Curtis dissimilarity matrices [33, 34]. The Bray–Curtis dissimilarity matrices were computed to measure the pairwise dissimilarity between samples, and PCoA was performed to ordinate the communities. Differences in beta diversity were further assessed using Analysis of Similarity (ANOSIM) [35], with Bonferroni corrections applied for multiple comparisons. All statistical analyses were performed at $\alpha = 0.05$ unless otherwise adjusted for multiple comparisons.

3 Results

3.1 Mice with AKPS tumors demonstrated tumor progression and metastasis

We first examined the differences in tumor progression between AKP (n = 9) and AKPS (n = 9) mice. Given the established role of SMAD4 as a regulator of epithelial-to-mesenchymal transition (EMT), we hypothesized that AKPS tumors would show more aggressive behavior than AKP tumors. To test this, we utilized an orthotopic injection model in which organoids with mutations in Apc, Kras, and p53 (AKP) or Apc, Kras, p53, and Smad4 (AKPS) were endoscopically implanted into the colon wall of C57BL/6 mice, and tumor progression was monitored over 8 weeks.

Our previous reports and other studies have suggested that AKPS organoids exhibit metastatic potential within 8 to 10 weeks [36, 37]. Interestingly, AKPS tumors showed metastasis to the lymph nodes, liver, or both in 6 out of 9 mice, whereas AKP tumors remained localized in the colon of all 9 mice. (Supplemental Fig. S1A). Histological analysis revealed significant differences in tumor morphology between the AKP and AKPS groups (Supplemental Fig. S1B). The AKP tumor models are differentiated, retaining some glandular features and exhibiting a more indolent growth pattern. In contrast, AKPS tumors are poorly differentiated, displaying high-grade features associated with loss of glandular architecture and increased malignancy. These findings align with the distinct metastatic potential of the AKPS model compared to the non-metastatic AKP model. Given the marked differences in metastatic potential and tumor histology, we next examined how the microbiome may be influenced by the presence or absence of the SMAD4 mutation over time.

3.2 Longitudinal changes in the gut microbial community of AKP tumor-bearing mice

We conducted a longitudinal examination of changes in the microbial community of AKP-tumor-bearing mice (n = 9) (Fig. 1**;** Composition and diversity of AKP microbiome). Between weeks 2 and 3, we observed an enrichment of *Faecalibaculum* and a concurrent decrease in the relative abundance of *Muribaculaceae* species (Fig. 1A). These shifts were accompanied by a temporal reduction in alpha diversity, as measured by the average Shannon index, between weeks 1 and 4 (Fig. 1B). To investigate overall compositional changes in the microbiome, we conducted principal coordinate analysis (PCoA) comparing the early stage (weeks 1–2) and late stage (weeks 3–8) phases of tumor progression. Although the animals were housed individually, microbiome compositions clustered distinctly by time point, showing significant differences between early and late stages, as measured by Bray–Curtis dissimilarity (ANOSIM $R = 0.6118$, $p < 0.001$) (Fig. 1C).

Next, we examined the correlation between specific bacterial taxa and the PCoA ordination positions to identify taxa linked to early versus late microbiome compositions. Spearman correlation analysis indicated that *Dubosiella* and *Akkermansia* were positively correlated with the early microbiome composition (Fig. 1D), while *Faecalibaculum* and *Paramuricaculum* were associated with the late-stage composition. Finally, we conducted the Kruskal–Wallis test to confirm changes in bacterial taxa between early and late compositions. We observed significant increases in *Faecalibaculum* ($p < 0.0001$) and decreases in *Dubosiella* ($p < 0.0001$) in the late-stage microbiome (Fig. 1E).

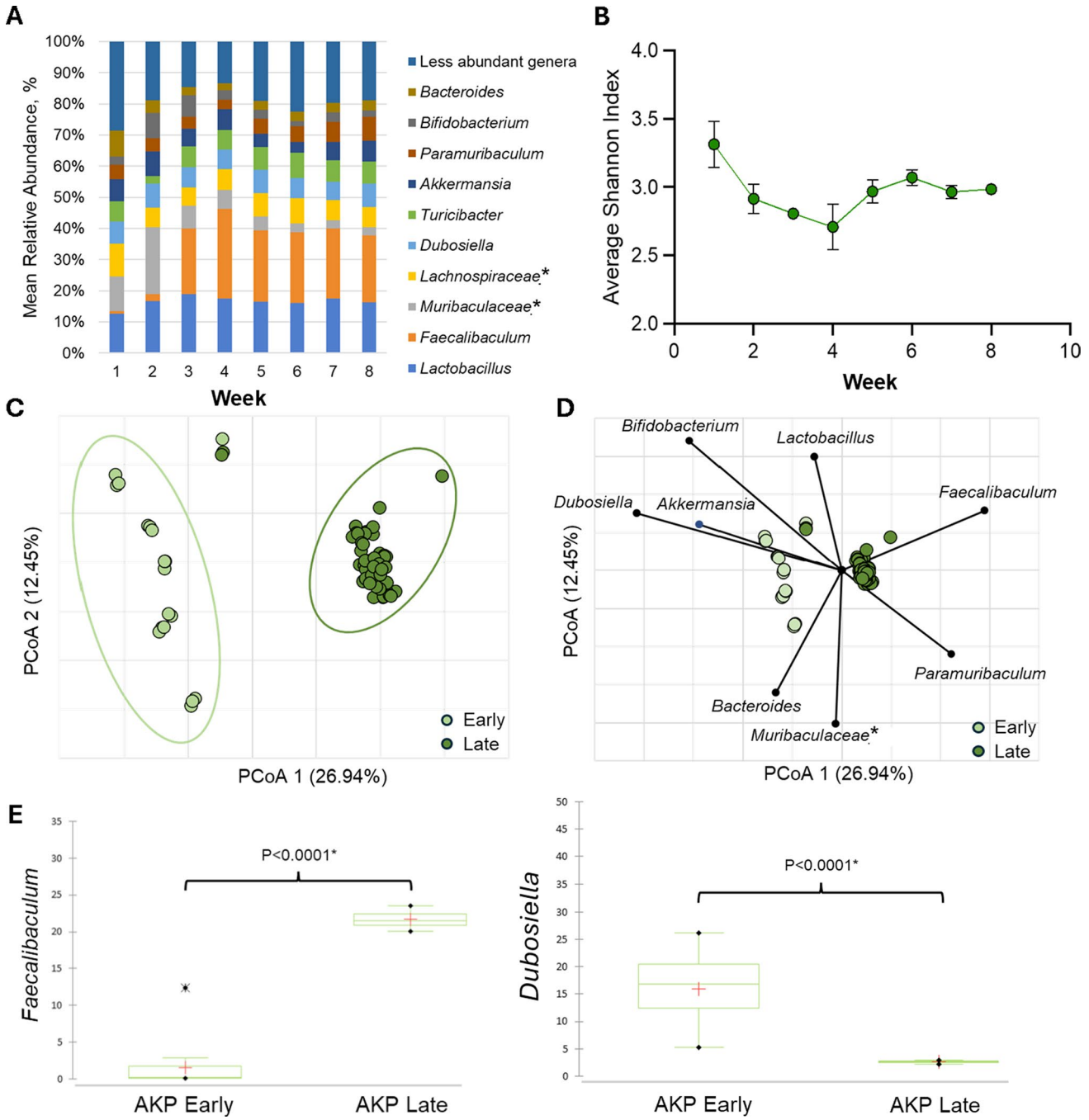

Fig. 1 Composition and diversity of AKP microbiome. **A** Longitudinal mean percent relative abundance of bacterial genera in AKP tumor-bearing mice. Genera that accounted for <0.07 of mean sequence reads were combined for clarity. (*) Indicates genera that could not be further classified. **B** Longitudinal average Shannon index for AKP tumor-bearing mice. **C** Principal Coordinates Analysis of early (Week 1–Week 2) and late (Week 3–Week 8) microbial compositions. **D** Correlated taxa with ordination positions on either axis (Spearman < 0.05) are overlaid on the PCoA plot. **E** Kruskal–Wallis comparison of selected bacterial genera (*Faecalibaculum and Dubosiella*) between AKP early (Week 1–2) and AKP late (Week 3–8). (*$p < 0.005$)

3.3 Longitudinal analysis of gut microbial community shifts in AKPS tumor-bearing mice

We performed a longitudinal study of microbial community changes in AKPS tumor-bearing mice (n = 9) over 8 weeks (Fig. 2**;** AKPS microbiome composition and diversity). Between weeks 2 and 3, we observed an enrichment

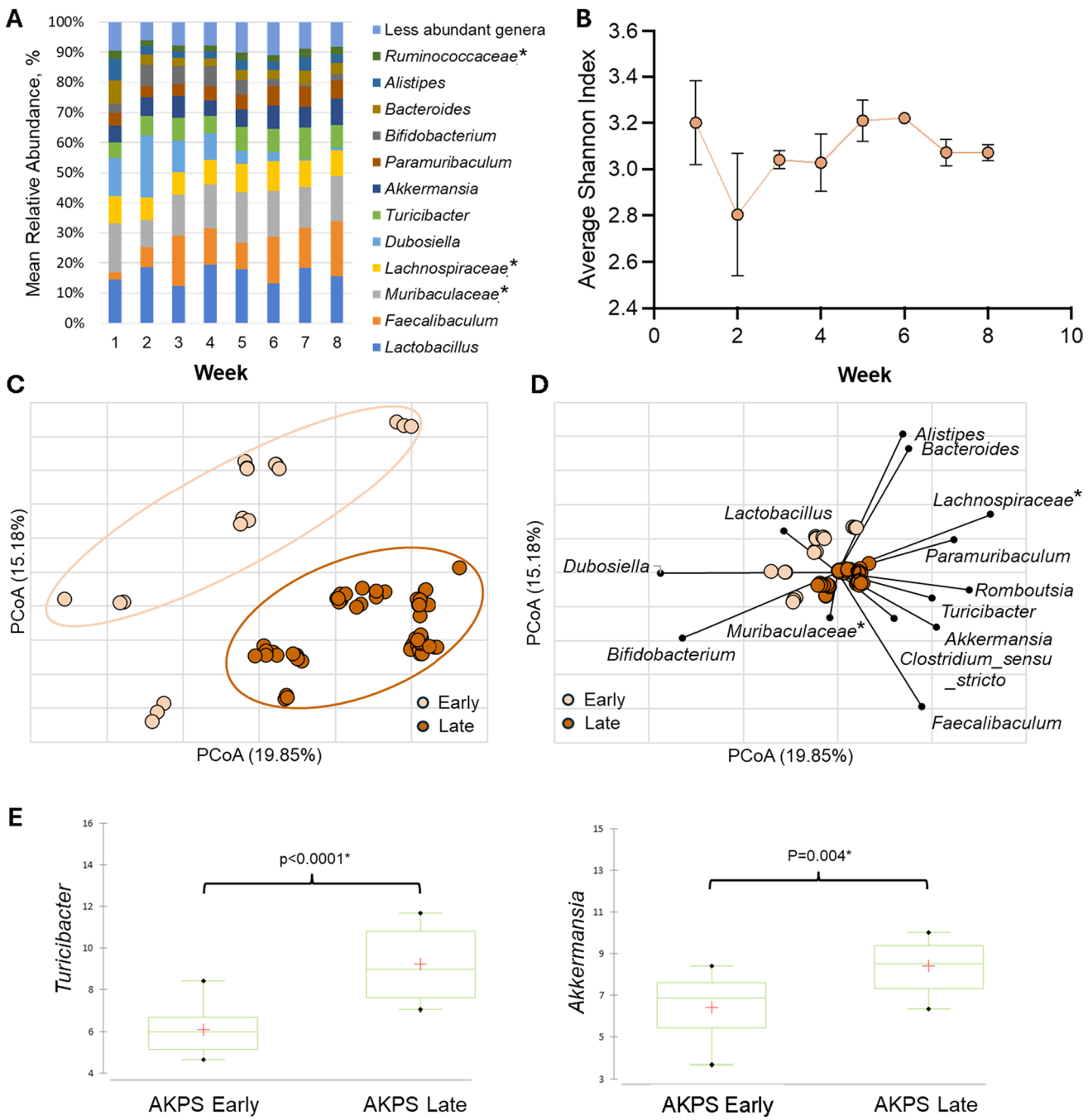

Fig. 2 AKPS microbiome composition and diversity. **A** Longitudinal mean percent relative abundance of bacterial genera in AKPS tumor-bearing mice. Genera that accounted for <0.07 of mean sequence reads were consolidated for clarity. (*) Indicates genera that could not be classified further. **B** Longitudinal average Shannon index for AKPS tumor-bearing mice. **C** Principal Coordinates Analysis of Early (Week 1–Week 2) and Late (Week 3–Week 8) microbial compositions. **D** Correlated taxa with ordination positions on either axis (Spearman < 0.05) are overlaid on the PCoA plot. (*) Indicates genera that could not be classified further. **E** Kruskal–Wallis comparison of selected bacterial genera (*Turicibacter and Akkermansia*) between AKPS Early (Week 1–2) and AKPS Late (Week 3–Week 8). (*$p < 0.005$)

of *Faecalibaculum* and a decrease in the relative abundance of *Dubosiella* (Fig. 2A). These microbial shifts coincided with temporal changes in alpha diversity, measured by the Shannon index, which showed a decrease between weeks 1 and 2, followed by an increase between weeks 2 and 6 (Fig. 2B). To assess overall compositional shifts, we performed PCoA to compare early (weeks 1–2) and late (weeks 3–8) time points. Despite individual housing, significant clustering of microbiome compositions was observed, revealing a marked difference in microbial profiles between the early and late stages of tumor progression (Bray–Curtis dissimilarity, ANOSIM R = 0.5835, $p < 0.001$) (Fig. 2C).

Next, we identified specific taxa correlated with the early and late microbiome compositions. *Dubosiella* and *Lactobacillus* were compositionally associated with the early stage (Fig. 2D), while *Faecalibaculum*, *Turicibacter*, *Romboutsia*, and *Akkermansia* were correlated with the late stage. Kruskal–Wallis tests confirmed significant increases in *Turicibacter* ($p < 0.0001$) and *Akkermansia* ($p < 0.0001$) between the early and late compositions (Fig. 2E).

3.4 Microbial diversity and composition differ between AKP and AKPS tumors

We compared the longitudinal changes in the mean relative abundance of microbial taxa between AKP and AKPS tumor-bearing mice (Fig. 3**;** Comparative microbiome composition and diversity of AKP and AKPS). Both groups exhibited similar trends, with *Faecalibaculum* increasing and *Dubosiella* decreasing as the tumors progressed (Fig. 3A). To assess the differences in microbiome diversity between the two groups, we analyzed alpha diversity. No significant differences were found during weeks 1–2; however, from weeks 3–8, AKPS mice displayed significantly higher Shannon Index values compared to AKP mice (Fig. 3B). There were no significant differences in Chao1 values between the groups (Supplemental Fig. S2).

We next assessed differences in community composition between AKP and AKPS tumors using Bray–Curtis dissimilarity (Fig. 3B). No significant differences were observed between early AKP and AKPS tumor communities (ANOSIM $R = 0.0447$, $p = 0.125$) (Fig. 3C). However, the microbiome composition of late-stage AKP tumors differed significantly from that of AKPS tumors (ANOSIM $R = 0.3725$, $p < 0.001$) (Fig. 3C). To identify bacterial genera associated with early and late-stage tumors, we performed a Spearman correlation analysis and plotted significant genera on a PCoA (Fig. 3D). Early-stage AKP and AKPS tumors were associated with the genera *Dubosiella*, *Akkermansia*, *Bacteroides*, and *Alistipes*. In contrast, late-stage AKP tumors correlated with *Faecalibaculum*. In contrast, late-stage AKPS tumors showed strong correlations with *Paramuribaculum* and *Muribaculaceae*_spp.

To further investigate the differences in bacterial abundance between AKP and AKPS tumors, we conducted a Kruskal–Wallis test (Fig. 3E). We observed contrasting trends in *the* abundance of Akkermansia in AKP tumor-bearing mice. *Akkermansia* decreased from early to late stages ($p = 0.059$), whereas, in AKPS mice, *Akkermansia* increased over time ($p = 0.004$). Additionally, *the* abundance of Akkermansia was significantly higher in mice with late-stage AKPS tumors compared to those with late-stage AKP tumors ($p < 0.0001$). Details of significantly altered taxa between early and late stages are provided in Supplemental Fig. S3.

Finally, we examined longitudinal changes in bacterial genera using the SplinectomeR permuspliner function (Fig. 4; Longitudinally significant genera between AKP and AKPS tumor-bearing mice). We identified significant longitudinal changes in the abundance of several genera, including Dubosiella ($p = 0.01$), Faecalibaculum ($p = 0.01$), Muribaculaceae_unclassified ($p = 0.01$), Lachnospiraceae_unclassified ($p = 0.01$), Turicibacter ($p = 0.03$), Akkermansia ($p = 0.01$), Paramuribaculum ($p = 0.01$), Bifidobacterium ($p = 0.01$), Clostridium_sensu_stricto ($p = 0.01$), and Romboutsia ($p = 0.01$).

4 Discussion

Our study provides novel insights into the role of the microbiome in tumor progression and metastasis in colorectal cancer (CRC), focusing on the differential impacts of the SMAD4 mutation. We compared microbial community changes between AKP and AKPS tumor-bearing mice, utilizing a comprehensive longitudinal approach that tracked microbiome shifts over time in relation to tumor progression. Our findings reveal that the microbiome undergoes significant compositional changes in response to the SMAD4 mutation, providing critical insights into how tumor mutations affect the gut microbial profile.

Our study revealed that AKPS tumor-bearing mice developed metastases in distant organs, including lymph nodes, liver, and lungs, while AKP tumors remained confined to the colon. This finding supports the hypothesis that SMAD4 loss increases tumor aggressiveness, given that SMAD4 is a crucial regulator of epithelial-to-mesenchymal transition, a critical process for metastasis. Notably, the microbial composition in AKPS tumors differed significantly from that in AKP tumors, particularly during the later stages of tumor progression, as shown by principal coordinate analysis (PCoA) and Bray–Curtis dissimilarity analysis. These changes suggest that microbial dysbiosis in the AKPS model may contribute to metastatic spread by modulating immune responses or altering the tumor microenvironment to facilitate the invasion and colonization of distant organs.

A key finding of our study is the distinct differences in microbial composition between AKP and AKPS tumor-bearing mice. Both groups showed similar trends in *Faecalibaculum* enrichment and *Dubosiella* reduction as tumors progressed. However, longitudinal shifts in microbiome diversity were more pronounced in AKPS tumors, with significantly higher

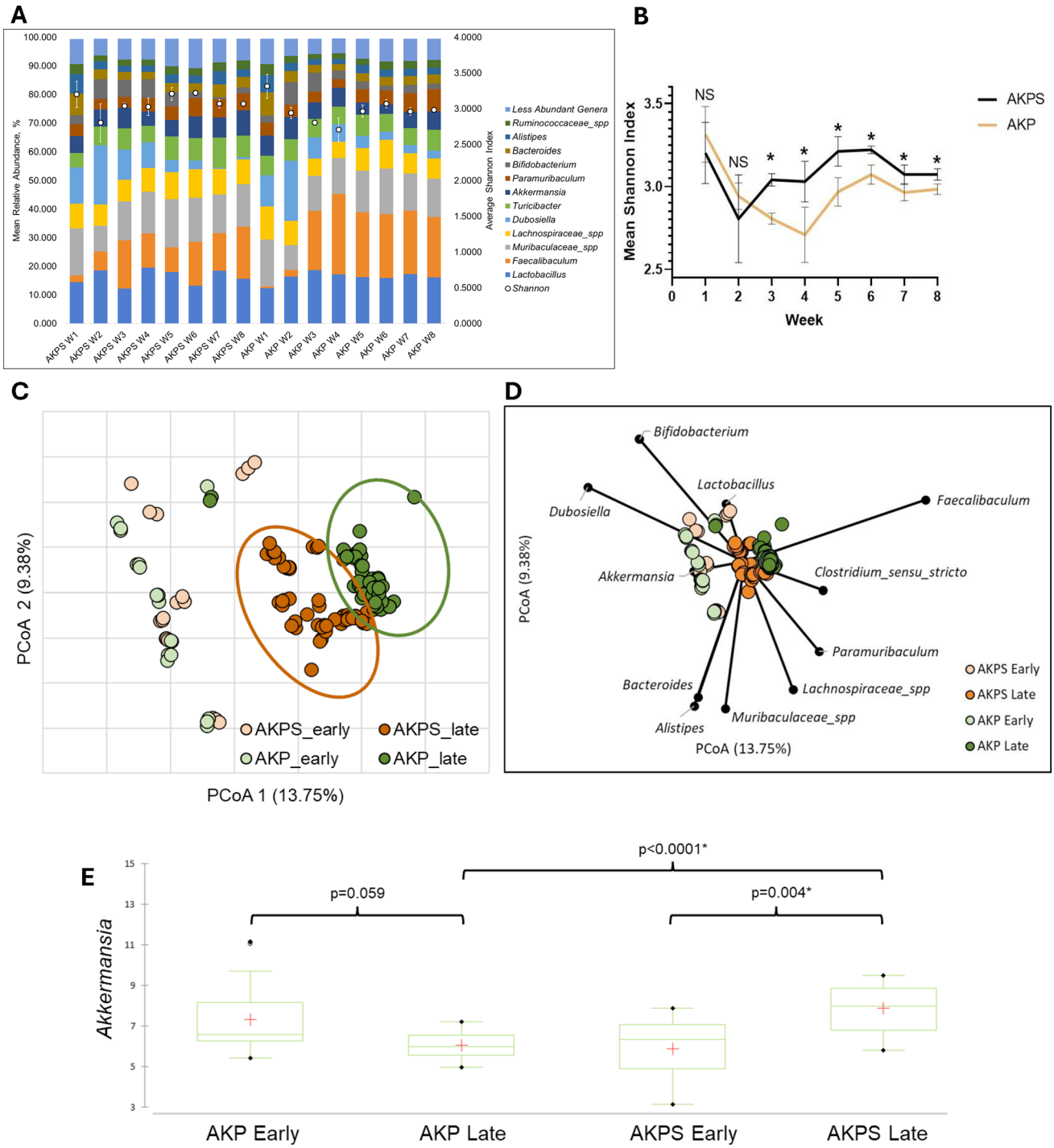

Fig. 3 Comparative microbiome composition and diversity of AKP and AKPS. **A** Longitudinal mean percent relative abundance of bacterial genera in tumor-bearing AKP and AKPS mice. Genera accounting for <0.07 of mean sequence reads were consolidated for clarity. (*) Indicates genera that could not be further classified. **B** Longitudinal average Shannon index for AKPS tumor-bearing mice. **C** Principal Coordinates Analysis of early (Week 1–Week 2) and late (Week 3–Week 8) microbial compositions. **D** Taxa correlated with ordination position on either axis (Spearman < 0.05) are overlaid on the PCoA plot. **E** Kruskal–Wallis comparison of *Akkermansia* between AKPS Early (Week 1–2) and AKPS Late (Week 3–Week 8). (*$p < 0.005$)

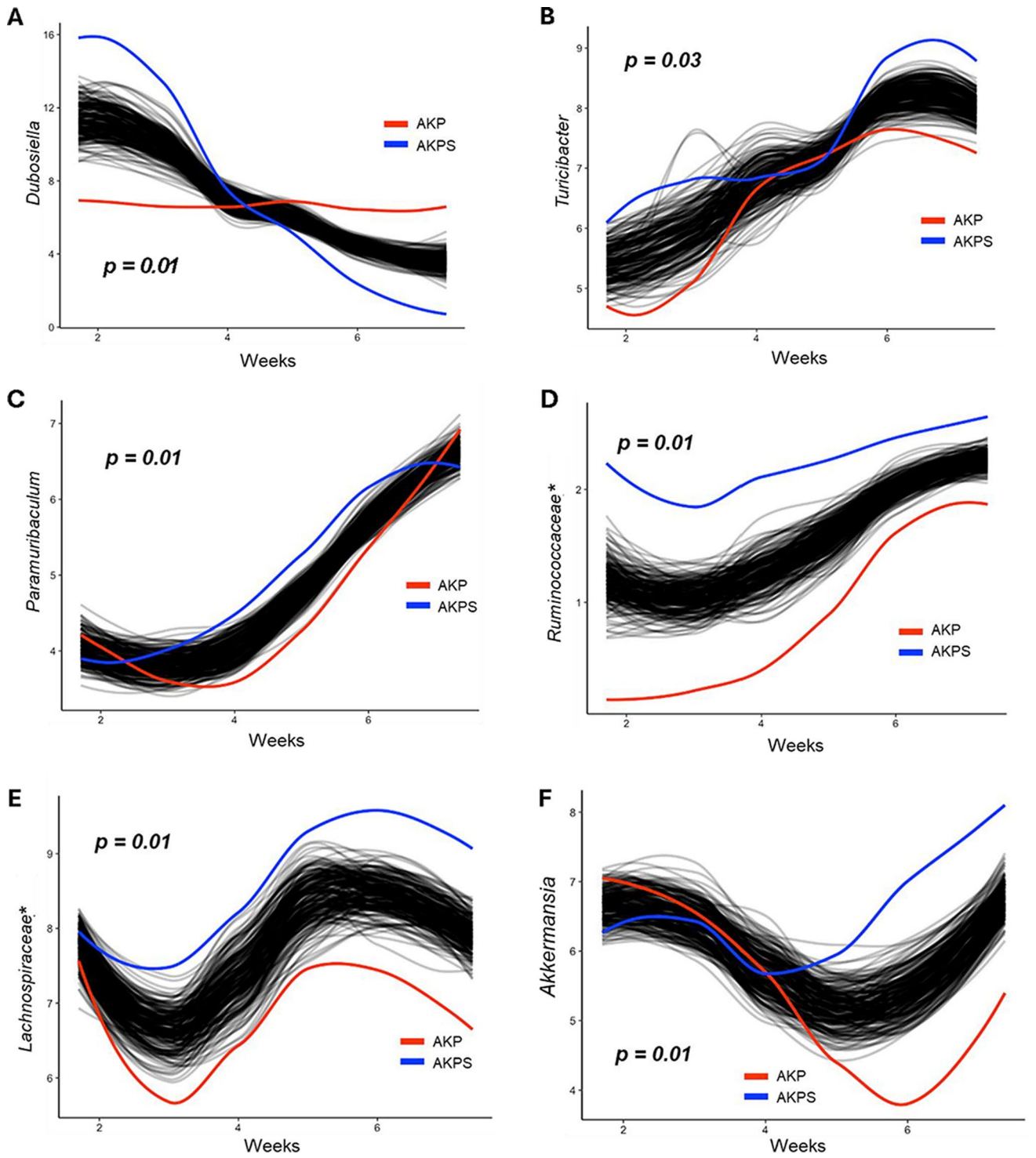

Fig. 4 Longitudinally significant genera between AKP and AKPS tumor-bearing mice. Longitudinal differences in the relative abundance of significantly different genera between AKP (*Red*) and AKPS (*Blue*) tumor-bearing mice, as determined by SplinectomeR, include: **A** *Dubosiella* ($p = 0.01$), **B** *Turicibacter* ($p = 0.03$), **C** *Paramuribaculum* ($p = 0.01$), **D** *Ruminococcaceae* ($p = 0.01$), **E** *Lachnospiraceae* ($p = 0.01$), and **F** *Akkermansia* ($p = 0.01$). (*) Indicates genera that could not be further classified

Shannon index values observed between weeks 3 and 8. This suggests that SMAD4 loss may increase microbial complexity within the TME and potentially influence tumor behavior.

These findings align with emerging evidence linking specific microbial taxa to more aggressive forms of CRC. While *Faecalibaculum* and *Dubosiella* were key genera in both models, their temporal changes and associations with tumor

progression differed between AKP and AKPS mice. *Faecalibaculum* showed a stronger correlation with AKPS tumors in later stages, potentially contributing to immune modulation or promoting an inflammatory environment that favors metastasis. In contrast, *Dubosiella* displayed a significant decrease in AKPS tumors, indicating its potential as a biomarker for less aggressive tumor types; its depletion may be associated with the loss of tumor-suppressive effects or microbial balance. Moreover, *Dubosiella* has been linked to protective immune-suppressive effects in CRC [38, 39], suggesting complex interactions between microbial taxa and the immune environment in CRC progression.

The genus *Bacteroides*, known for colonizing mucus and preventing gut dysbiosis by outcompeting pathogens [40], showed a declining trend in both AKP and AKPS tumors as they progressed. This aligns with previous findings linking reduced *Bacteroides* abundance to CRC pathogenesis [41]. *Bacteroides* have been associated with suppressing tumor progression by producing polysaccharide A, which modulates immune responses and maintains gut homeostasis [42, 43]. Its depletion in AKPS tumors, especially those that metastasize, suggests it could serve as a protective agent against tumor advancement and may therefore represent a potential therapeutic target.

In contrast, *Bifidobacterium*, which is typically found at low levels in CRC patients [44, 45], increased in abundance over time in both AKP and AKPS tumors. This genus produces lactic acid and acetate—metabolites associated with immune modulation and tumor growth [46–48]. In cases of colitis, *Bifidobacterium* has been shown to enhance mitochondrial metabolism in regulatory T cells (Tregs) [49]. While Tregs are generally associated with immunosuppression in various cancers, the role of Tregs in CRC has yielded mixed results [50, 51]. The observed increase in *Bifidobacterium* may contribute to an immunosuppressive microenvironment, thereby promoting tumor progression and metastasis.

Several genera associated with butyrate and short-chain fatty acid (SCFA) production were more abundant in AKPS tumors than in AKP tumors, including *Lachnospiraceae spp.* and *Ruminococcaceae spp.* Notably, *Lachnospiraceae spp.* was consistently present across early to late stages in AKPS samples. Butyrate, produced by these genera, has been shown to modulate inflammatory and immune responses, often promoting an immunosuppressive state [52–54]. In *APC*-mutated mice, butyrate secretion has also been linked to tumorigenesis [55].

We also found *Muribaculaceae spp.* to be more abundant in AKPS tumors than in AKP tumors, although its abundance decreased from early to late stages. *Muribaculaceae* produces propionate as a metabolic byproduct and is associated with mucosal repair [56]. Higher *Muribaculaceae* levels have been inversely correlated with inflammation and carcinogenesis, suggesting its potential protective role in maintaining gut homeostasis and modulating the tumor microenvironment [57].

The correlation of specific taxa with early- versus late-stage tumor composition reveals important dynamics in the tumor-associated microbiome. For example, *Akkermansia* displayed opposing trends in AKP versus AKPS tumors, with its abundance decreasing in AKP tumors but increasing in AKPS tumors over time. This divergence suggests that *Akkermansia* could serve as a dynamic microbiome marker associated with tumor progression and aggressiveness. The increased presence of *Akkermansia* in late-stage AKPS tumors, particularly in those with metastatic potential, hints at its potential role in promoting metastasis—possibly through modulation of immune checkpoints or alteration of systemic inflammatory responses. *Akkermansia*, a mucin-degrading bacterium, is often elevated in CRC patients [58, 59]. In our previous studies using the AOM/DSS model of inflammation-driven CRC (id-CRC), we found that fecal microbiota restoration from healthy control mice led to increased *Akkermansia* levels, which corresponded to transient decreases in lipocalin-2, an inflammatory marker in the intestine [60]. This suggests that *Akkermansia* may have context-dependent roles, influencing tumor progression through immune modulation and interactions with inflammatory pathways.

Additionally, *Lachnospiraceae* spp., recognized for their butyrate production, were more abundant in AKPS tumors, highlighting the potential immunosuppressive effects linked to SCFA production. Butyrate influences inflammatory responses in ways that may promote tumor progression [54]. The enrichment of these microbial genera in AKPS tumors suggests that SMAD4 loss may drive the development of a tumor-supportive microbiome that aids in tumor progression and metastasis by modulating immune responses and inflammatory pathways.

4.1 Limitations and future directions

While our findings provide valuable insights into the relationship between microbiome dynamics and tumor progression, several limitations must be acknowledged. This study was conducted using preclinical mouse models, which, although highly informative, do not fully recapitulate the genetic heterogeneity, microbial diversity, and tumor microenvironment found in human CRC. Therefore, validation in human CRC cohorts is essential to confirm the clinical relevance of our observations.

Additionally, we used only female mice to reduce biological variability; however, sex-specific differences in microbiome composition and immune responses may influence CRC progression in humans. Future studies should include both male and female models to more effectively account for potential sex-dependent effects.

Our study primarily focused on longitudinal microbiome changes in the presence and absence of the SMAD4 mutation, establishing correlations between microbial composition and tumor progression. However, a more integrated analysis that incorporates metabolomics and immune profiling would provide deeper mechanistic insights into microbiome-tumor interactions, particularly regarding tumor metabolism and the immune landscape. Furthermore, interventional studies utilizing microbiome-modulating approaches, such as antibiotic treatment or fecal microbiota transplantation (FMT), will be essential to clarify the mechanistic role and determine whether specific microbial shifts actively drive tumor progression or are merely bystander effects of tumor evolution.

5 Conclusion

In summary, this study demonstrates that CRC progression is influenced by longitudinal alterations in the microbiome, with distinct shifts occurring in response to the addition of the SMAD4 mutation. These findings provide novel insights into how specific microbial taxa contribute to tumor progression and metastasis, highlighting their potential as biomarkers or therapeutic targets in clinical settings.

Acknowledgements We thank the core facilities of the Masonic Cancer Center and the Clinical and Translational Sciences Institute for their support of histological services. This study is funded by research grants from the Minnesota Colorectal Cancer Funds and the Mezin-Koats Colon Cancer Research Fund.

Author contributions All authors provided meaningful intellectual contributions to this work and were involved in its preparation and editing. TJG, DW, and SS conceived the study. TJG, DW, KMBB, BK, CS, and SS generated and analyzed the data. TJG, KMBB, BK, and SS wrote the manuscript, and all the authors edited it.

Funding This study was supported by research grants from the Mezin-Koats Colon Cancer Research Fund and the Minnesota Colorectal Cancer Funds.

Data availability Raw datasets as Fastq files are available on the NCBI server; https://www.ncbi.nlm.nih.gov/sraPRJNA988535

Declarations

Ethics approval and consent to participate This study adhered to the University of Minnesota Institutional Animal Care and Use Committee protocol code 2107-39273A.

Competing interests The authors declare no competing interests.

References

1. Siegel RL, Giaquinto AN, Jemal A. Cancer statistics, 2024. CA Cancer J Clin. 2024;74(1):12–49. https://doi.org/10.3322/caac.21820.
2. Hofseth LJ, Hebert JR, Chanda A, Chen H, Love BL, Pena MM, et al. Early-onset colorectal cancer: initial clues and current views. Nat Rev Gastroenterol Hepatol. 2020;17(6):352–64. https://doi.org/10.1038/s41575-019-0253-4.
3. Wu CW, Lui RN. Early-onset colorectal cancer: current insights and future directions. World J Gastrointest Oncol. 2022;14(1):230–41. https://doi.org/10.4251/wjgo.v14.i1.230.
4. Shaukat A, Kahi CJ, Burke CA, Rabeneck L, Sauer BG, Rex DK. ACG Clinical Guidelines: Colorectal Cancer Screening 2021. Am J Gastroenterol. 2021;116(3):458–79. https://doi.org/10.14309/ajg.0000000000001122.
5. Cercek A, Chatila WK, Yaeger R, Walch H, Fernandes GDS, Krishnan A, et al. A comprehensive comparison of early-onset and average-onset colorectal cancers. J Natl Cancer Inst. 2021;113(12):1683–92. https://doi.org/10.1093/jnci/djab124.

6. Connell LC, Mota JM, Braghiroli MI, Hoff PM. The rising incidence of younger patients with colorectal cancer: questions about screening, biology, and treatment. Curr Treat Options Oncol. 2017;18(4):23. https://doi.org/10.1007/s11864-017-0463-3.
7. Smit WL, Spaan CN, Johannes de Boer R, Ramesh P, Martins Garcia T, Meijer BJ, et al. Driver mutations of the adenoma-carcinoma sequence govern the intestinal epithelial global translational capacity. Proc Natl Acad Sci. 2020;117(41):25560–70. https://doi.org/10.1073/pnas.1912772117.
8. Zhang L, Shay JW. Multiple roles of APC and its therapeutic implications in colorectal cancer. J Natl Cancer Inst. 2017;109(8):djw332. https://doi.org/10.1093/jnci/djw332.
9. Zhu G, Pei L, Xia H, Tang Q, Bi F. Role of oncogenic KRAS in the prognosis, diagnosis and treatment of colorectal cancer. Mol Cancer. 2021;20(1):143. https://doi.org/10.1186/s12943-021-01441-4.
10. Dinu D, Dobre M, Panaitescu E, Bîrlă R, Iosif C, Hoara P, et al. Prognostic significance of KRAS gene mutations in colorectal cancer–preliminary study. J Med Life. 2014;7(4):581–7.
11. Hassin O, Nataraj NB, Shreberk-Shaked M, Aylon Y, Yaeger R, Fontemaggi G, et al. Different hotspot p53 mutants exert distinct phenotypes and predict outcome of colorectal cancer patients. Nat Commun. 2022;13(1):2800. https://doi.org/10.1038/s41467-022-30481-7.
12. Li XL, Zhou J, Chen ZR, Chng WJ. P53 mutations in colorectal cancer - molecular pathogenesis and pharmacological reactivation. World J Gastroenterol. 2015;21(1):84–93. https://doi.org/10.3748/wjg.v21.i1.84.
13. Massagué J, Blain SW, Lo RS. TGFbeta signaling in growth control, cancer, and heritable disorders. Cell. 2000;103(2):295–309. https://doi.org/10.1016/s0092-8674(00)00121-5.
14. Zhang B, Halder SK, Kashikar ND, Cho YJ, Datta A, Gorden DL, et al. Antimetastatic role of Smad4 signaling in colorectal cancer. Gastroenterology. 2010;138(3):969-80.e1-3. https://doi.org/10.1053/j.gastro.2009.11.004.
15. Mehta RS, Nishihara R, Cao Y, Song M, Mima K, Qian ZR, et al. Association of dietary patterns with risk of colorectal cancer subtypes classified by *Fusobacterium nucleatum* in tumor tissue. JAMA Oncol. 2017;3(7):921–7. https://doi.org/10.1001/jamaoncol.2016.6374.
16. Liu PH, Wu K, Ng K, Zauber AG, Nguyen LH, Song M, et al. Association of obesity with risk of early-onset colorectal cancer among women. JAMA Oncol. 2019;5(1):37–44. https://doi.org/10.1001/jamaoncol.2018.4280.
17. Song M, Chan AT, Sun J. Influence of the gut microbiome, diet, and environment on risk of colorectal cancer. Gastroenterology. 2020;158(2):322–40. https://doi.org/10.1053/j.gastro.2019.06.048.
18. Wong CC, Yu J. Gut microbiota in colorectal cancer development and therapy. Nat Rev Clin Oncol. 2023;20(7):429–52. https://doi.org/10.1038/s41571-023-00766-x.
19. Montalban-Arques A, Scharl M. Intestinal microbiota and colorectal carcinoma: implications for pathogenesis, diagnosis, and therapy. EBioMedicine. 2019;48:648–55. https://doi.org/10.1016/j.ebiom.2019.09.050.
20. Allen J, Rosendahl Huber A, Pleguezuelos-Manzano C, Puschhof J, Wu S, Wu X, et al. Colon Tumors in Enterotoxigenic *Bacteroides fragilis* (ETBF)-colonized mice do not display a unique mutational signature but instead possess host-dependent alterations in the APC gene. Microbiol Spectr. 2022;10(3): e0105522. https://doi.org/10.1128/spectrum.01055-22.
21. Haghi F, Goli E, Mirzaei B, Zeighami H. The association between fecal enterotoxigenic *B. fragilis* with colorectal cancer. BMC Cancer. 2019;19(1):879. https://doi.org/10.1186/s12885-019-6115-1.
22. Okuda S, Shimada Y, Tajima Y, Yuza K, Hirose Y, Ichikawa H, et al. Profiling of host genetic alterations and intra-tumor microbiomes in colorectal cancer. Comput Struct Biotechnol J. 2021;19:3330–8. https://doi.org/10.1016/j.csbj.2021.05.049.
23. Yuan D, Tao Y, Wang H, Wang J, Cao Y, Cao W, et al. A comprehensive analysis of the microbiota composition and host driver gene mutations in colorectal cancer. Invest New Drugs. 2022;40(5):884–94. https://doi.org/10.1007/s10637-022-01263-1.
24. Liang S, Mao Y, Liao M, Xu Y, Chen Y, Huang X, et al. Gut microbiome associated with APC gene mutation in patients with intestinal adenomatous polyps. Int J Biol Sci. 2020;16(1):135–46. https://doi.org/10.7150/ijbs.37399.
25. Wang Z, Hopson LM, Singleton SS, Yang X, Jogunoori W, Mazumder R, et al. Mice with dysfunctional TGF-β signaling develop altered intestinal microbiome and colorectal cancer resistant to 5FU. Biochim Biophys Acta Mol Basis Dis. 2021;1867(10): 166179. https://doi.org/10.1016/j.bbadis.2021.166179.
26. Sato T, Vries RG, Snippert HJ, van de Wetering M, Barker N, Stange DE, et al. Single Lgr5 stem cells build crypt-villus structures in vitro without a mesenchymal niche. Nature. 2009;459(7244):262–5. https://doi.org/10.1038/nature07935.
27. Schloss PD, Westcott SL, Ryabin T, Hall JR, Hartmann M, Hollister EB, et al. Introducing mothur: open-source, platform-independent, community-supported software for describing and comparing microbial communities. Appl Environ Microbiol. 2009;75(23):7537–41. https://doi.org/10.1128/aem.01541-09.
28. Aronesty E. Comparison of sequencing utility programs. Open Bioinformatics J. 2013;7:1–8.
29. Pruesse E, Quast C, Knittel K, Fuchs BM, Ludwig W, Peplies J, et al. SILVA: a comprehensive online resource for quality checked and aligned ribosomal RNA sequence data compatible with ARB. Nucleic Acids Res. 2007;35(21):7188–96. https://doi.org/10.1093/nar/gkm864.
30. Huse SM, Welch DM, Morrison HG, Sogin ML. Ironing out the wrinkles in the rare biosphere through improved OTU clustering. Environ Microbiol. 2010;12(7):1889–98. https://doi.org/10.1111/j.1462-2920.2010.02193.x.
31. Edgar RC, Haas BJ, Clemente JC, Quince C, Knight R. UCHIME improves sensitivity and speed of chimera detection. Bioinformatics. 2011;27(16):2194–200. https://doi.org/10.1093/bioinformatics/btr381.
32. Cole JR, Wang Q, Cardenas E, Fish J, Chai B, Farris RJ, et al. The Ribosomal Database Project: improved alignments and new tools for rRNA analysis. Nucleic Acids Res. 2009;37:D141–5. https://doi.org/10.1093/nar/gkn879.
33. Anderson MJ, Willis TJ. Canonical analysis of principal coordinates: a useful method of constrained ordination for ecology. Ecology. 2003;84(2):511–25. https://doi.org/10.1890/0012-9658(2003)084.
34. Bray JR, Curtis JT. An ordination of the upland forest communities of Southern Wisconsin. Ecol Monogr. 1957;27(4):325–49. https://doi.org/10.2307/1942268.
35. Clarke KR. Non-parametric multivariate analyses of changes in community structure. Aust J Ecol. 1993;18(1):117–43. https://doi.org/10.1111/j.1442-9993.1993.tb00438.x.
36. Wangmo D, Gates TJ, Zhao X, Sun R, Subramanian S. Centrosomal Protein 55 (CEP55) drives immune exclusion and resistance to immune checkpoint inhibitors in colorectal cancer. Vaccines (Basel). 2024;12(1):63. https://doi.org/10.3390/vaccines12010063.

37. Westcott PMK, Sacks NJ, Schenkel JM, Ely ZA, Smith O, Hauck H, et al. Low neoantigen expression and poor T-cell priming underlie early immune escape in colorectal cancer. Nat Cancer. 2021;2(10):1071–85. https://doi.org/10.1038/s43018-021-00247-z.
38. Zhang Y, Tu S, Ji X, Wu J, Meng J, Gao J, et al. Dubosiella newyorkensis modulates immune tolerance in colitis via the L-lysine-activated AhR-IDO1-Kyn pathway. Nat Commun. 2024;15(1):1333. https://doi.org/10.1038/s41467-024-45636-x.
39. Sui H, Zhang L, Gu K, Chai N, Ji Q, Zhou L, et al. YYFZBJS ameliorates colorectal cancer progression in Apc(Min/+) mice by remodeling gut microbiota and inhibiting regulatory T-cell generation. Cell Commun Signal. 2020;18(1):113. https://doi.org/10.1186/s12964-020-00596-9.
40. Zafar H, Saier MH Jr. Gut Bacteroides species in health and disease. Gut Microbes. 2021;13(1):1–20. https://doi.org/10.1080/19490976.2020.1848158.
41. Cao Y, Shang F, Jin M, Deng S, Gu J, Mao F, et al. Changes in Bacteroides and the microbiota in patients with obstructed colorectal cancer: retrospective cohort study. BJS Open. 2023;7(6):zrad105. https://doi.org/10.1093/bjsopen/zrad105.
42. Mazmanian SK, Liu CH, Tzianabos AO, Kasper DL. An immunomodulatory molecule of symbiotic bacteria directs maturation of the host immune system. Cell. 2005;122(1):107–18. https://doi.org/10.1016/j.cell.2005.05.007.
43. Lee YK, Mehrabian P, Boyajian S, Wu WL, Selicha J, Vonderfecht S, et al. The protective role of *Bacteroides fragilis* in a murine model of colitis-associated colorectal cancer. mSphere. 2018;3(6):587–618. https://doi.org/10.1128/mSphere.00587-18.
44. Loftus M, Hassouneh SA, Yooseph S. Bacterial community structure alterations within the colorectal cancer gut microbiome. BMC Microbiol. 2021;21(1):98. https://doi.org/10.1186/s12866-021-02153-x.
45. Kosumi K, Hamada T, Koh H, Borowsky J, Bullman S, Twombly TS, et al. The amount of Bifidobacterium genus in colorectal carcinoma tissue in relation to tumor characteristics and clinical outcome. Am J Pathol. 2018;188(12):2839–52. https://doi.org/10.1016/j.ajpath.2018.08.015.
46. Rivière A, Selak M, Lantin D, Leroy F, De Vuyst L. Bifidobacteria and butyrate-producing colon bacteria: importance and strategies for their stimulation in the human gut. Front Microbiol. 2016;7:979. https://doi.org/10.3389/fmicb.2016.00979.
47. Schug ZT, Vande Voorde J, Gottlieb E. The metabolic fate of acetate in cancer. Nat Rev Cancer. 2016;16(11):708–17. https://doi.org/10.1038/nrc.2016.87.
48. Fukuda S, Toh H, Taylor TD, Ohno H, Hattori M. Acetate-producing bifidobacteria protect the host from enteropathogenic infection via carbohydrate transporters. Gut Microbes. 2012;3(5):449–54. https://doi.org/10.4161/gmic.21214.
49. Sun S, Luo L, Liang W, Yin Q, Guo J, Rush AM, et al. Bifidobacterium alters the gut microbiota and modulates the functional metabolism of T regulatory cells in the context of immune checkpoint blockade. Proc Natl Acad Sci U S A. 2020;117(44):27509–15. https://doi.org/10.1073/pnas.1921223117.
50. Sinicrope FA, Rego RL, Ansell SM, Knutson KL, Foster NR, Sargent DJ. Intraepithelial effector (CD3+)/regulatory (FoxP3+) T-cell ratio predicts a clinical outcome of human colon carcinoma. Gastroenterology. 2009;137(4):1270–9. https://doi.org/10.1053/j.gastro.2009.06.053.
51. Salama P, Phillips M, Grieu F, Morris M, Zeps N, Joseph D, et al. Tumor-infiltrating FOXP3+ T regulatory cells show strong prognostic significance in colorectal cancer. J Clin Oncol. 2009;27(2):186–92. https://doi.org/10.1200/jco.2008.18.7229.
52. Millard AL, Mertes PM, Ittelet D, Villard F, Jeannesson P, Bernard J. Butyrate affects differentiation, maturation and function of human monocyte-derived dendritic cells and macrophages. Clin Exp Immunol. 2002;130(2):245–55. https://doi.org/10.1046/j.0009-9104.2002.01977.x.
53. Zimmerman MA, Singh N, Martin PM, Thangaraju M, Ganapathy V, Waller JL, et al. Butyrate suppresses colonic inflammation through HDAC1-dependent Fas upregulation and Fas-mediated apoptosis of T cells. Am J Physiol Gastrointest Liver Physiol. 2012;302(12):G1405–15. https://doi.org/10.1152/ajpgi.00543.2011.
54. Chang PV, Hao L, Offermanns S, Medzhitov R. The microbial metabolite butyrate regulates intestinal macrophage function via histone deacetylase inhibition. Proc Natl Acad Sci U S A. 2014;111(6):2247–52. https://doi.org/10.1073/pnas.1322269111.
55. Okumura S, Konishi Y, Narukawa M, Sugiura Y, Yoshimoto S, Arai Y, et al. Gut bacteria identified in colorectal cancer patients promote tumourigenesis via butyrate secretion. Nat Commun. 2021;12(1):5674. https://doi.org/10.1038/s41467-021-25965-x.
56. Smith BJ, Miller RA, Schmidt TM. Muribaculaceae genomes assembled from metagenomes suggest genetic drivers of differential response to acarbose treatment in mice. mSphere. 2021;6(6):0085121. https://doi.org/10.1128/msphere.00851-21.
57. Jain T, Sharma P, Are AC, Vickers SM, Dudeja V. New insights into the cancer-microbiome-immune axis: decrypting a decade of discoveries. Front Immunol. 2021;12: 622064. https://doi.org/10.3389/fimmu.2021.622064.
58. Belzer C, de Vos WM. Microbes inside–from diversity to function: the case of Akkermansia. Isme j. 2012;6(8):1449–58. https://doi.org/10.1038/ismej.2012.6.
59. Weir TL, Manter DK, Sheflin AM, Barnett BA, Heuberger AL, Ryan EP. Stool microbiome and metabolome differences between colorectal cancer patients and healthy adults. PLoS ONE. 2013;8(8): e70803. https://doi.org/10.1371/journal.pone.0070803.
60. Gates TJ, Yuan C, Shetty M, Kaiser T, Nelson AC, Chauhan A, et al. Fecal microbiota restoration modulates the microbiome in inflammation-driven colorectal cancer. Cancers (Basel). 2023;15(8):2260. https://doi.org/10.3390/cancers15082260.